Proc. of the Second Intl. Conf. on Advances in Civil, Structural and Construction Engineering - CSCE 2015

ISBN: 978-1-63248-042-2 doi: 10.15224/ 978-1-63248-042-2-01

The Effects of Viscous Bulk Compressibility for Noncylindrical Helices

Nihal Eratlı, Hakan Argeso, Mehmet H. Omurtag

***Abstract*—In this study, the effects of viscous bulk compressibility on the dynamic viscoelastic response of noncylindrical helicoidal rods are examined. For this aim, a viscoelastic model is proposed that takes standard type of distortional behavior and Kelvin type of bulk compressibility. Based on Timoshenko beam theory, two-nodded curvilinear elements are in Laplace space. The viscoelastic material properties are implemented into the formulation through the use of the correspondence principle (elastic-viscoelastic analogy). The analysis is carried out in the Laplace space and the results are transformed back to time space numerically by using the modified Durbin's algorithm. As sample problems, the noncylindrical helicoidal rods fixed from both ends which are subjected to dynamic step type of distributed loading are considered. Three different helicoidal rods that have different helical geometries are analyzed and their dynamic responses are compared. The effects of viscous bulk compressibility are also investigated.**

***Keywords*—viscoelasticity, noncylindrical helicoidal rod, mixed finite element method, Laplace space**

I. Introduction

Generally, helicoidal rods appear to be one of the critical elements within engineering structures due to their functionality. The proper design of these elements must be fulfilled after performing a reliable analysis. This fact becomes more important if these elements are subjected to dynamic loading.

It is a common practice to analyze the dynamic response of engineering structures by assuming that the material is linearly elastic. However, there may be some cases that, the viscous effects arising from the internal friction within these structures could not be neglected.

The theory of viscoelasticity is well established and many textbooks about this topic are available in literature such as [1,2]. The viscoelastic behaviors of straight and circular bars were examined extensively [3-9], however, few studies exist in literature that investigates the viscoelastic behavior of helicoidal bars [10-13]. Within these studies the works that takes helicoidal bars having noncircular cross section into account are even more rare.

Nihal Eratlı (Assoc. Professor)[1]
Department of Civil Engineering, Istanbul Technical University, Turkey

Hakan Argeso (Assoc. Professor)[2]
Department of Manufacturing Engineering, Atılım University, Turkey

Mehmet H. Omurtag (Professor)[3]
Department of Civil Engineering, Istanbul Technical University, Turkey

When the material exhibits linear viscoelastic behavior, the correspondence principle can be used for the analysis [14]. This principle states that the field equations of the viscoelastic problem in the Laplace space may be obtained from those for the elastic problem by replacing the elastic constants with complex moduli according to the chosen viscoelastic models.

Within the scope of this study, the dynamic behavior of linear viscoelastic noncylindrical helical rods having square cross section is investigated. For this aim, a mixed finite element formulation based on Timoshenko beam theory is used, and, element matrices for two nodded curvilinear space rod element are obtained in Laplace space. The new viscoelastic material properties are inserted into the finite element algorithm verified by [12]. It is assumed that, the material exhibits standard type of distortional behavior and Kelvin type of bulk compressibility. The complex moduli associated with these material models are implemented in the formulation via the correspondence principle. The solution of the system matrices of finite element method are carried out in Laplace space. Then, the results obtained in Laplace space are transformed back to time space with the use of Modified Durbin's algorithm [15-17]. Helicoidal rods that have different helical geometries are considered. These rods are assumed to be fixed from both ends and subjected to dynamic step type of vertical distributed loading. Analyses are performed for investigating the influence of the helix geometry and the effects of viscous bulk compressibility on the dynamic response of helicoidal rods.

II. Formulation

A. The Helix Geometry

The geometry of a helix can be defined in the Cartesian coordinate system in terms of the helix parameters as: $x = R(\varphi)\cos\varphi$, $y = R(\varphi)\sin\varphi$ and $z = p(\varphi)\varphi$, where $p(\varphi) = R(\varphi)\tan\alpha$. Here, α is the pitch angle. $p(\varphi)$ is a function of the horizontal angle φ and defines the step for unit angle of the helix. For the conical helix geometry (Type I), the centerline radius $R(\varphi)$ is expressed as

$$R(\varphi) = R_1 + \frac{(R_2 - R_1)\varphi}{2n\pi} \tag{1}$$

and for the barrel (Type II) and hyperboloidal (Type III) helix geometries, $R(\varphi)$ is

Proc. of the Second Intl. Conf. on Advances in Civil, Structural and Construction Engineering - CSCE 2015

ISBN: 978-1-63248-042-2 doi: 10.15224/ 978-1-63248-042-2-01

$$R(\varphi) = R_2 + (R_1 - R_2)\left(1 - \frac{\varphi}{2n\pi}\right)^2 \qquad (2)$$

where n is the number of active turns. Here, as examples, R_1 and R_2 are shown for noncylindrical helical geometries in Figure 1.

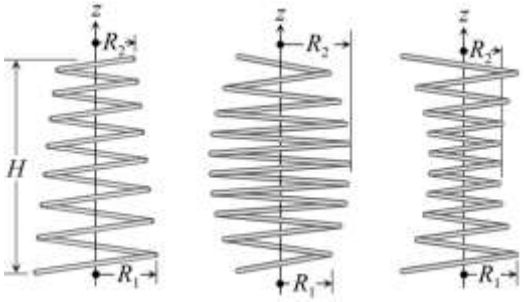

Figure 1. Conical, barrel and hyperboloidal helix geometries

B. *The Field Equations and Functional in the Laplace Space*

The field equations of the elastic cylindrical/non-cylindrical helix based on the Timoshenko beam assumptions were presented by [18] regarding Frenet coordinate system. Based on this premise, the Laplace transformed field equations can be listed as follows:

$$\begin{aligned} -\bar{\mathbf{T}}_{,s} - \bar{\mathbf{q}} + \rho A z^2 \bar{\mathbf{u}} &= \mathbf{0} \\ -\bar{\mathbf{M}}_{,s} - \mathbf{t}\times\bar{\mathbf{T}} - \bar{\mathbf{m}} + \rho \mathbf{I} z^2 \bar{\mathbf{\Omega}} &= \mathbf{0} \\ \bar{\mathbf{u}}_{,s} + \mathbf{t}\times\bar{\mathbf{\Omega}} - \bar{\mathbf{C}}_\gamma \bar{\mathbf{T}} &= \mathbf{0} \\ \bar{\mathbf{\Omega}}_{,s} - \bar{\mathbf{C}}_\kappa \bar{\mathbf{M}} &= \mathbf{0} \end{aligned} \qquad (3)$$

where the Laplace transformed variables are denoted by the over bars, comma as a subscript under the variable designates the differentiation with respect to s and z is the Laplace transformation parameter. In (3), $\bar{\mathbf{u}}(\bar{u}_t, \bar{u}_n, \bar{u}_b)$ is the displacement vector, $\bar{\mathbf{\Omega}}(\bar{\Omega}_t, \bar{\Omega}_n, \bar{\Omega}_b)$ is the rotation vector, $\bar{\mathbf{T}}(\bar{T}_t, \bar{T}_n, \bar{T}_b)$ is the force vector, $\bar{\mathbf{M}}(\bar{M}_t, \bar{M}_n, \bar{M}_b)$ is the moment vector in the Laplace space, ρ is the density of homogeneous material, A is the area of the cross section, $\mathbf{I}(I_t, I_n, I_b)$ is the moment of inertia of the cross section, $\bar{\mathbf{q}}$ and $\bar{\mathbf{m}}$ are the distributed external force and moment vectors in the Laplace space, $\bar{\mathbf{C}}_\gamma$ and $\bar{\mathbf{C}}_\kappa$ are the compliance matrices in the Laplace space, namely,

$$\bar{\mathbf{C}}_\kappa = \begin{bmatrix} 1/\bar{G}I_t & 0 & 0 \\ 0 & 1/\bar{E}I_n & 0 \\ 0 & 0 & 1/\bar{E}I_b \end{bmatrix} \quad \bar{\mathbf{C}}_\gamma = \begin{bmatrix} 1/\bar{E}A & 0 & 0 \\ 0 & 1/\bar{G}A & 0 \\ 0 & 0 & 1/\bar{G}A \end{bmatrix} \qquad (4)$$

where $A' = A/k'$ and k' is the shear correction factor. (3) is written in the operator form $\mathbf{Q} = \mathbf{L}\mathbf{y} - \mathbf{f}$, if the operator is potential, the equality $\left\langle \mathrm{d}\mathbf{Q}(\mathbf{y}, \bar{\mathbf{y}}), \mathbf{y}^* \right\rangle = \left\langle \mathrm{d}\mathbf{Q}(\mathbf{y}, \mathbf{y}^*), \bar{\mathbf{y}} \right\rangle$ must be satisfied [19]. $\mathrm{d}\mathbf{Q}(\bar{\mathbf{y}}, \hat{\mathbf{y}})$ and $\mathrm{d}\mathbf{Q}(\bar{\mathbf{y}}, \bar{\mathbf{y}}^*)$ are Gâteaux derivatives of the operator in directions of $\hat{\mathbf{y}}$ and $\bar{\mathbf{y}}^*$. After proving the operator to be potential, the functional of the structural problem is obtained in the Laplace space as follows [12]:

$$\begin{aligned} \mathbf{I}(\bar{\mathbf{y}}) = &-[\bar{\mathbf{u}}, \bar{\mathbf{T}}_{,s}] + [\mathbf{t}\times\bar{\mathbf{\Omega}}, \bar{\mathbf{T}}] - [\bar{\mathbf{M}}_{,s}, \bar{\mathbf{\Omega}}] - \tfrac{1}{2}[\mathbf{C}_\kappa \bar{\mathbf{M}}, \bar{\mathbf{M}}] \\ &- \tfrac{1}{2}[\mathbf{C}_\gamma \bar{\mathbf{T}}, \bar{\mathbf{T}}] + \tfrac{1}{2}\rho A z^2 [\bar{\mathbf{u}}, \bar{\mathbf{u}}] + \tfrac{1}{2}\rho z^2 [\mathbf{I}\bar{\mathbf{\Omega}}, \bar{\mathbf{\Omega}}] \\ &- [\bar{\mathbf{q}}, \bar{\mathbf{u}}] - [\bar{\mathbf{m}}, \bar{\mathbf{\Omega}}] + [(\bar{\mathbf{T}} - \hat{\bar{\mathbf{T}}}), \bar{\mathbf{u}}]_\sigma + [(\bar{\mathbf{M}} - \hat{\bar{\mathbf{M}}}), \bar{\mathbf{\Omega}}]_\sigma \\ &+ [\hat{\bar{\mathbf{u}}}, \bar{\mathbf{T}}]_\varepsilon + [\hat{\bar{\mathbf{\Omega}}}, \bar{\mathbf{M}}]_\varepsilon \end{aligned} \qquad (5)$$

The terms with hats in (5) define the known values on the boundary. The subscripts ε and σ , represent the geometric and dynamic boundary conditions, respectively.

C. *Mixed Finite Element Formulation*

A two nodded curved element is used to discretize the beam domain. Linear shape functions $\phi_i = (\varphi_j - \varphi)/\Delta\varphi$ and $\phi_j = (\varphi - \varphi_i)/\Delta\varphi$ are employed in the mixed finite element formulation where $\Delta\varphi = (\varphi_j - \varphi_i)$. The curvatures are satisfied exactly at the nodal points and linearly interpolated through the element [12]. Each node has 12 degrees of freedom namely:

$$\mathbf{X}^T = \{\bar{u}_t, \bar{u}_n, \bar{u}_b, \bar{\Omega}_t, \bar{\Omega}_n, \bar{\Omega}_b, \bar{T}_t, \bar{T}_n, \bar{T}_b, \bar{M}_t, \bar{M}_n, \bar{M}_b\} \qquad (6)$$

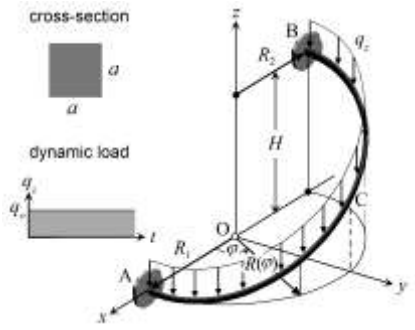

Figure 2. The helicoidal rod with both ends fixed

III. Numerical Examples

Helicoidal rods having different helical geometries that are analyzed in this study are shown in Figures 3, 4 and 5 (Type I, Type II and Type III). These rods are assumed to be fixed from both ends and subjected to dynamic step type of vertical distributed loading that have an intensity of $q_o = 10\text{N/m}$ (See Figure 2). The helix geometries are defined by making use of (1) and (2). The helix geometry has $n = 0.5$ number of active

Proc. of the Second Intl. Conf. on Advances in Civil, Structural and Construction Engineering - CSCE 2015

ISBN: 978-1-63248-042-2 doi: 10.15224/ 978-1-63248-042-2-01

turns, the height of the rod is $H = 3\text{m}$ and the minimum radius of helix to maximum radius of helix ratios $R_{\min} / R_{\max} = 0.5$ where $R_{\max} = 2\text{m}$. The square cross-sectional area of the rod is $A = 400\text{cm}^2$. The material density is $\rho = 1000\ \text{kg/m}^3$.

(a) Three dimensional view (b) Top view
Figure 3 Helicoidal rod: Type I

(a) Three dimensional view (b) Top view
Figure 4 Helicoidal rod: Type II

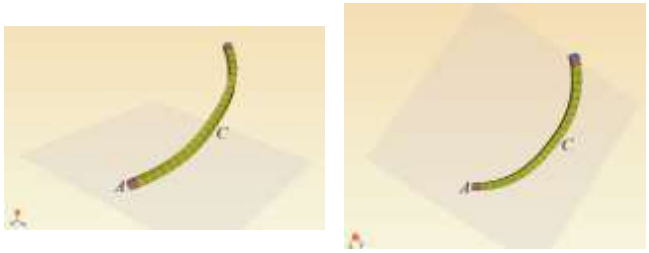

(a) Three dimensional view (b) Top view
Figure 5 Helicoidal rod: Type III

As stated, we assume that the material exhibits standard type of distortional behavior and Kelvin type of bulk compressibility. The form of complex shear modulus can be expressed as

$$\bar{G} = G\left[(\beta^G - 1)\frac{z}{z + 1/\tau_r^G} + 1\right] \quad ; \beta^G = G_g / G > 1 \qquad (7)$$

where, τ_r^G , G and G_g are the retardation time, the equilibrium value and the instantaneous value of relaxation function associated with shear modulus. In the analyses, we select $G = 7\times10^5\ \text{N/m}^2$, $\tau_r^G = 0.01\text{s}$ and $\beta^G = 3$. The form of complex bulk modulus is given by

$$\bar{K} = K\left[1 + z\,\overset{*}{\tau}{}_r^K\right] \qquad (8)$$

where $\overset{*}{\tau}{}_r^K$ and K are the retardation time and the equilibrium value of creep function associated with bulk modulus. In order to the investigate the effects of viscous bulk compressibility on the dynamic behavior, we select $K = 1.5167\times10^6\ \text{N/m}^2$ and perform the analyses for $\overset{*}{\tau}{}_r^K = 0.0\text{s}; 0.1\text{s}; 0.5\text{s}; 1.0\text{s}$. We note that, when $\overset{*}{\tau}{}_r^K = 0.0\text{s}$ the material exhibits elastic bulk compressibility.

Helicoidal rods are discretized by using 40 elements and the solutions of system matrices of the finite element method are carried out in Laplace space. The results are transformed back to time space by making use of modified Durbin's algorithm [12].

Time variations of the vertical displacement u_z evaluated at the mid points (see point C in Figure 2) between $0 \le t \le 50\text{s}$ for three types of helicoidal rods are shown in Figures 6a, 6b and 6c, respectively. Each figure contains four different results that correspond to different values of retardation times of bulk modulus. From each figure, one may observe that, as the values of $\overset{*}{\tau}{}_r^K$ increase (the viscous effects associated with the bulk compressibility increase), the magnitude of u_z decreases and also u_z damps quicker. Plots for the time variations of the moment M_y evaluated at the fixed end (see point A in Figure 2) of the rods are depicted in Figures 7a, 7b and 7c. The time variations of M_y also show a similar behavior as those of u_z .

Figures 8a and 8b, respectively, compare the time variations of u_z and M_y determined for three different helicoidal rods having different helical geometries. The retardation time associated with bulk modulus is taken as $\overset{*}{\tau}{}_r^K = 0.1\text{s}$. Observation of the responses from these figures reveals that, the amplitudes of u_z and M_y obtained for Type II are significantly higher than those corresponding to Type I and Type III. On the other hand, Type II has the lower vibration frequency for both responses when compared with the other. We see that, the amplitudes of u_z and M_y obtained for Type III are lower than those corresponding to Type I and Type II. Especially, the difference in u_z is significant. We also note that, the responses determined for Type III have the highest vibration frequencies.

IV. Conclusions

Using a viscoelastic material model which takes standard type of distortional behavior and Kelvin type of bulk compressibility into account, linear viscoelastic noncylindrical helicoidal rods are analyzed by using mixed finite element method. The formulation is accomplished in Laplace space and the viscoelastic material properties are accounted through the use of correspondence principle. The analyses are carried out in Laplace space and then the results are transformed back

Proc. of the Second Intl. Conf. on Advances in Civil, Structural and Construction Engineering - CSCE 2015

ISBN: 978-1-63248-042-2 doi: 10.15224/ 978-1-63248-042-2-01

to time space via Modified Durbin's algorithm. Three helicoidal rods that have different types of helical geometries are analyzed. The influence of the helix geometry and the effects of viscous bulk compressibility on the dynamic response for these helicoidal rods are discussed extensively.

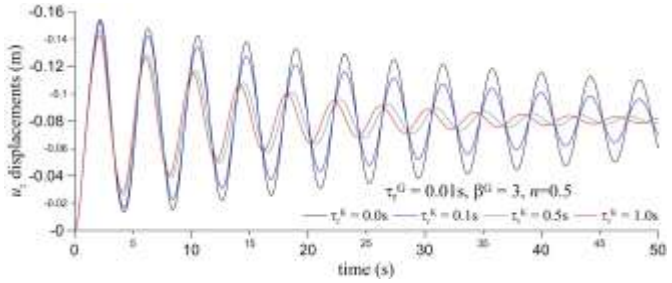

(a) Type I

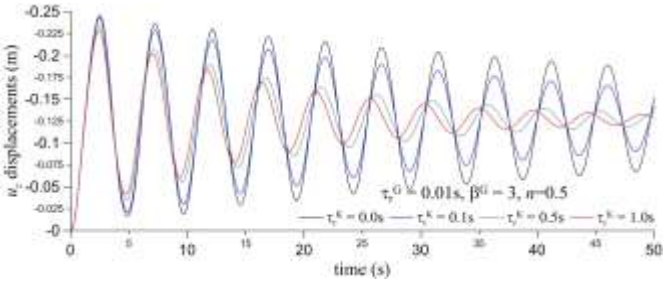

(b) Type II

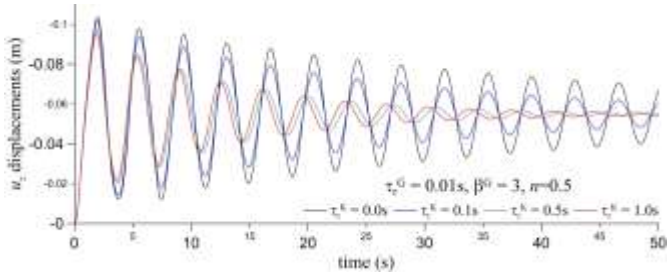

(c) Type III

Figure 6. Comparison of the time variations of u_z for the helicoidal rods having different grades of viscous bulk compressibility

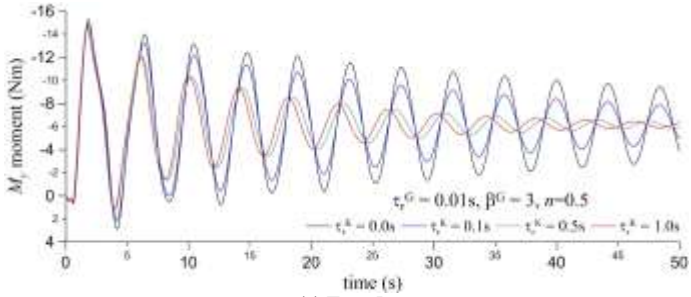

(a) Type I

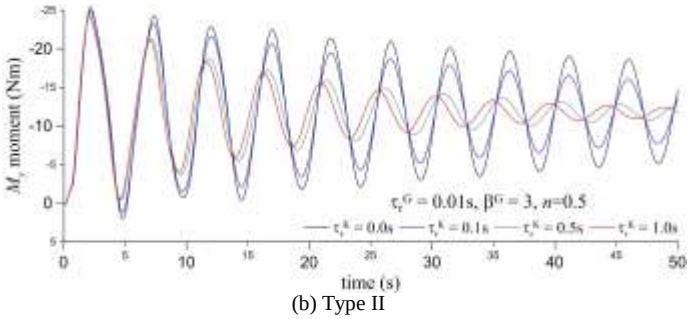

(b) Type II

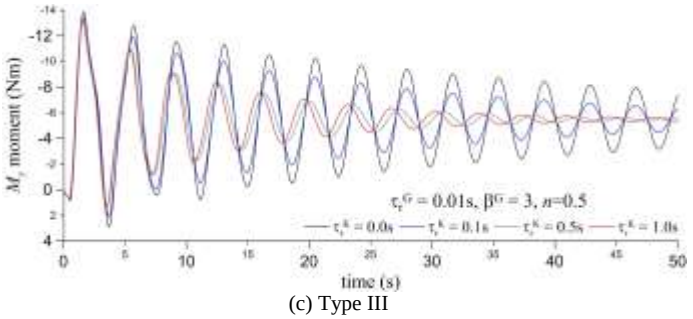

(c) Type III

Figure 7. Comparison of the time variations of M_y for the helicoidal rods having different grades of viscous bulk compressibility

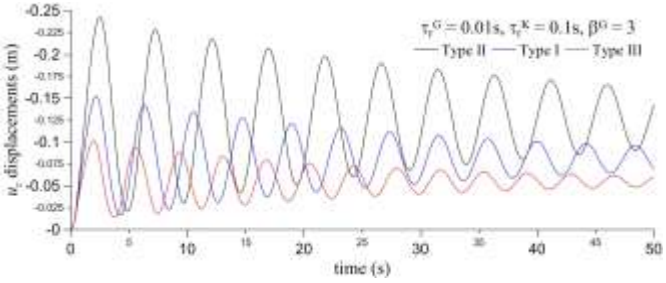

(a) u_z

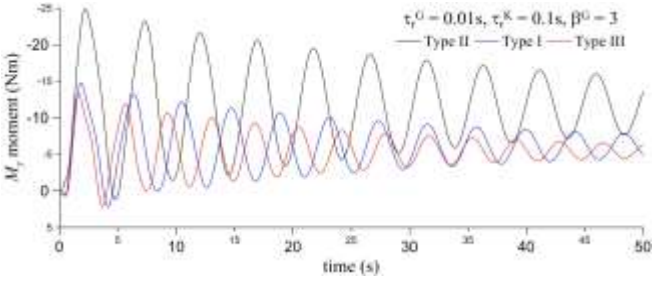

(b) M_y

Figure 8. Comparison of the time variations of u_z and M_y for three different types of helicoidal rods

ISBN: 978-1-63248-042-2 doi: 10.15224/ 978-1-63248-042-2-01

Acknowledgment

This research is supported by The Scientific and Technological Research Council of Turkey under project no 111M308. This support is gratefully acknowledged by the authors.

References

[1] W. Flügge, Viscoelasticity, Springer Berlin Heidelberg, 1975.
[2] R. Christensen, Theory of Viscoelasticity: An Introduction, Elsevier, 1982.
[3] W.H. Chen, T.C. Lin, Dynamic analysis of viscoelastic structure using incremental finite element method, Eng. Struct. 4 (1982) 271–276.
[4] T. Chen, The hybrid Laplace transform/finite element method applied to the quasi-static and dynamic analysis of viscoelastic Timoshenko beams, Int. J. Numer. Methods Eng. 38 (1995) 509–522.
[5] C.M. Wang, T.Q. Yang, K.Y. Lam, Viscoelastic Timoshenko beam solutions form Euler-Bernoulli solutions, J. Eng. Mech.-ASCE 123 (1997) 746–748.
[6] Y. Aköz, F. Kadıoğlu, The mixed finite element method for the quasi-static and dynamic analysis of viscoelastic Timoshenko beams, Int. J. Numer. Methods Eng. 44 (1999) 1909–1932.
[7] T. Kocatürk, M. Şimşek, Dynamic analysis of eccentrically prestressed viscoelastic Timoshenko beams under a moving harmonic load, Comput. Struct. 84 (31-32) (2006) 2113–2127.
[8] T. Kocatürk, M. Şimşek, Vibration of viscoelastic beams subjected to an eccentric compressive force and a concentrated moving harmonic force, J. Sound Vib. 291(1-2) (2006) 302–322.
[9] G.S. Payette, J.N. Reddy, Nonlinear quasi-static finite element formulations for viscoelastic Euler-Bernoulli and Timoshenko beams, Int. J. for Numer. Methods in Biomedical Eng. 26 (2010) 1736–1755.
[10] B. Temel, Transient analysis of viscoelastic helical rods subject to time-dependent loads, Int. J. Solids Struct. 41 (2004) 1605–1624.
[11] B. Temel, F.F. Çalım, N. Tütüncü, Quasi-static and dynamic response of viscoelastic helical rods, J. Sound Vib. 271 (2004) 921–935.
[12] N. Eratlı, H. Argeso, F.F. Çalım, B. Temel, M.H. Omurtag, Dynamic analysis of linear viscoelastic cylindrical and conical helicoidal rods using the mixed FEM, J. Sound Vib. 333 (2014) 3671–3690.
[13] N. Eratlı, Kutlu, A., Dynamic behavior of the viscoelastic non-cylindrical helices with a mixed finite element formulation, 2nd International Conference on Advances in Civil, Structural and Environmental Engineering-ACSEE, Zurich, Switzerland (2014) 61–64.
[14] B.A. Boley, J.H. Weiner, Theory of Thermal Stresses, Courier Dover Publications, 1960.
[15] H. Dubner, J. Abate, Numerical inversion of Laplace transforms by relating them to the finite Fourier cosine transform, J ACM. 15 (1968) 115–123.
[16] F. Durbin, Numerical inversion of Laplace transforms: An efficient improvement to Dubner and Abate's method, Comput. J. 17 (1974) 371–376.
[17] G. Narayanan, Numerical Operational Methods in Structural Dynamics, Ph.D., University of Minnesota, 1980.
[18] M.H. Omurtag, A.Y. Aköz, The mixed finite element solution of helical beams with variable cross-section under arbitrary loading, Comput. Struct. 43 (1992) 325–331.
[19] J.T. Oden, J.N. Reddy, Variational Methods in Theoretical Mechanics, Springer, 1976.